at UCSB. Research at UCSB was supported by a United States National Science Foundation grant to P.C.F.

Registry No. $Rh(NH_3)_5Cl^{2+}$, 15379-09-6; $Rh(ND_3)_5Cl^{2+}$, 50513-49-0; $Rh(NH_3)_5Br^{2+}$, 15337-80-1; $Rh(ND_3)_5Br^{2+}$, 50513-50-3; $Rh(NH_3)_5H_2O^{3+}$, 15337-79-8; *trans*-$Rh(NH_3)_4(H_2O)Cl^{2+}$, 38781-25-8; $Rh(ND_3)_5D_2O^{3+}$, 83967-60-6; *trans*-$Rh(ND_3)_4(D_2O)Cl^{2+}$, 83967-61-7; *trans*-$Rh(NH_3)_4(H_2O)Br^{2+}$, 71424-39-0; *trans*-$Rh(ND_3)_4(D_2O)Br^{2+}$, 83967-62-8; Cl^-, 16887-00-6; NH_4^+, 14798-03-9; Br^-, 24959-67-9.

Contribution from the School of Chemical Sciences, University of Illinois, Urbana, Illinois 61801, and the Department of Chemistry, University of Colorado, Boulder, Colorado 80309

Magnetic Exchange Interactions Propagated by Saturated Bridges in Binuclear Dicyclopentadienyltitanium(III) Complexes

ARRIETTA W. CLAUSS,[1] SCOTT R. WILSON,[1] ROBERT M. BUCHANAN,[2] CORTLANDT G. PIERPONT,[2] and DAVID N. HENDRICKSON*[1]

Received August 23, 1982

The single-crystal X-ray structures of one mononuclear and two binuclear dicyclopentadienyltitanium(III) carboxylate complexes have been determined. The mononuclear benzoate complex $(\eta^5\text{-}C_5H_5)_2Ti(O_2CC_6H_5)$ crystallizes in space group $P2_1/n$ with $a = 11.388$ (2) Å, $b = 11.564$ (2) Å, $c = 22.673$ (3) Å, $\beta = 105.09$ (1)°, and $Z = 8$. Diffraction data were collected with a Syntex P$\bar{1}$ automated diffractometer, and the structure was refined to $R_F = 0.054$ and $R_{wF} = 0.059$ for 2257 reflections with $I > 3\sigma(I)$ and $2\theta = 3\text{-}50.0°$ (Mo Kα radiation). There are two independent $(\eta^5\text{-}C_5H_5)_2Ti(O_2CC_6H_5)$ molecules in the unit cell; both have similar bond distances and angles. The angles and distances within the titanium coordination sphere are those expected for pseudotetrahedral coordination. The dihedral angles between the phenyl rings of the benzoate ligands and the

planes in the two different molecules are 12.8 and 11.3°. The binuclear complex bridged by the bicyclo[1.1.1]pentane-1,3-dicarboxylate dianion, $(\eta^5\text{-}C_5H_5)_2Ti(O_2CC_5H_6CO_2)Ti(\eta^5\text{-}C_5H_5)_2$, crystallizes in the space group $P2_1/c$ with $a = 8.136$ (2) Å, $b = 10.671$ (2) Å, $c = 17.553$ (3) Å, $\beta = 124.4$ (1)°, and $Z = 4$. Diffraction data were collected with a Syntex $P2_1$ automated diffractometer, and the structure was refined to $R_F = 0.044$ and $R_{wF} = 0.061$ for 2083 reflections with $I > 3\sigma(I)$ and $2\theta = 3.5\text{-}55.0°$ (Mo Kα radiation). Normal pseudotetrahedral distances and angles are found for each of the Ti(III) ions in the binuclear complex. The binuclear complex is centrosymmetric with the bicyclo[1.1.1]pentane moiety disordered equally in two positions and with an *intra*molecular Ti-Ti distance of 9.8509 (6) Å. The nonbonding bridgehead C-C distance increases from 1.845 Å in bicyclo[1.1.1]pentane to 1.858 (4) Å in the dicarboxylate bridge of the binuclear complex. The binuclear complex bridged by the *trans*-cyclobutane-1,2-dicarboxylate dianion, $(\eta^5\text{-}C_5H_5)_2Ti(O_2CC_4H_6CO_2)Ti(\eta^5\text{-}C_5H_5)_2$, crystallizes in the orthorhombic space group $P2_12_12_1$ with $a = 11.096$ (2) Å, $b = 26.804$ (5) Å, $c = 8.049$ (1) Å, and $Z = 4$. Diffraction data were collected with a Syntex $P2_1$ automated diffractometer, and the structure was refined to $R_F = 0.038$ and $R_{wF} = 0.052$ for 2355 reflections with $I > 3\sigma(I)$ and $2\theta = 3.5\text{-}55.0°$ (Mo Kα radiation). The cyclobutane ring of the bridging dicarboxylate dianion is nonplanar with a dihedral angle of 153°. The *intra*molecular Ti-Ti distance in the cyclobutanedicarboxylate-bridged binuclear complex is 7.8326 (11) Å. The origin of the weak ($J = -3.9$ cm^{-1} with $H = -2JS_1 \cdot S_2$) antiferromagnetic exchange interaction for the "mononuclear" benzoate complex is examined with the X-ray results, as well as with characterization of analogous molecules such as $(\eta^5\text{-}C_5Me_5)_2Ti(O_2CC_6H_5)$. Variable-temperature (3-12 K) EPR results for toluene-benzene (4:1) glasses of five of the complexes, together with previously measured room-temperature EPR spectra, clearly indicate the presence of *intra*molecular magnetic exchange interactions in these binuclear dicyclopentadienyltitanium(III) complexes.

Introduction

In a series[3-5] of recent papers the question whether a saturated bridge could propagate a magnetic exchange interaction between two distant $(\eta^5\text{-}C_5H_5)_2Ti^{III}$ moieties was investigated. Sixteen binuclear complexes with saturated bridges and six with unsaturated bridges were examined. All 22 complexes are bridged by dicarboxylate dianions (where B is some hydrocarbon):

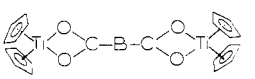

Titanium hyperfine observed in the *solution-state* EPR spectra for several of the binuclear complexes definitely established the presence of an *intra*molecular magnetic exchange interaction between the two Ti(III)-metallocene units. Antiferromagnetic exchange interactions ($J = -0.8$ to -3.0 cm^{-1}) were also evident in the magnetic susceptibility data for many of these complexes in the *solid-state*. It was difficult to decide whether the antiferromagnetic interaction seen for the solid-

(1) University of Illinois.
(2) University of Colorado.
(3) Francesconi, L. C.; Corbin, D. R.; Clauss, A. W.; Hendrickson, D. N.; Stucky, G. D. *Inorg. Chem.* **1981**, *20*, 2059.
(4) Kramer, L. S.; Clauss, A. W.; Francesconi, L. C.; Corbin, D. R.; Hendrickson, D. N.; Stucky, G. D. *Inorg. Chem.* **1981**, *20*, 2070.
(5) Francesconi, L. C.; Corbin, D. R.; Clauss, A. W.; Hendrickson, D. N.; Stucky, G. D. *Inorg. Chem.* **1981**, *20*, 2078.
(6) Campbell, S. J.; Herbert, I. R.; Warwick, C. B.; Woodgate, J. M. *Rev. Sci. Instrum.* **1976**, *47*, 1172.
(7) Wertz, J. E.; Bolton, J. R. In "Electron Spin Resonance: Elementary Theory and Practical Application"; McGraw-Hill: New York, 1972; p 34.
(8) Baseman, R. J.; Pratt, D. W.; Chow, M.; Dowd, P. *J. Am. Chem. Soc.* **1976**, *98*, 5726.
(9) Pierpont, C. G. *Inorg. Chem.* **1977**, *16*, 636.

0020-1669/83/1322-0628$01.50/0

Table I. Experimental Data for the X-ray Diffraction Studies

	$Cp_2TiO_2CC_6H_5$	$Cp_2TiO_2CC_4H_6CO_2TiCp_2$	$Cp_2TiO_2CC_5H_6CO_2TiCp_2$
	(A) Crystal Parameters		
cryst syst	monoclinic	orthorhombic	monoclinic
space group	$P2_1/n$	$P2_12_12_1$	$P2_1/c$
a, Å	11.388 (2)	11.096 (2)	8.136 (2)
b, Å	11.564 (2)	26.804 (5)	10.671 (2)
c, Å	22.673 (3)	8.049 (1)	17.553 (3)
β, deg	105.09 (1)		124.4 (1)
V, Å^3	2883.1 (7)	2393.9 (7)	1257.3 (5)
Z	8	4	4
fw	299.21	498.29	255.15
ρ(calcd) g cm^{-3}	1.378	1.382	1.348
μ, cm^{-1}	6.17	4.47	6.56
	(B) Measurement of Data		
diffractometer	Syntex $P\bar{1}$	Syntex $P2_1$	Syntex $P2_1$
radiation	Mo Kα (λ = 0.710 69 Å)		
monochromator	graphite		
2θ limits, deg	$3.0 \leq 2\theta \leq 50.0$	$3.5 \leq 2\theta \leq 55.0$	$3.5 \leq 2\theta \leq 55.0$
scan range, deg	±0.7	−0.8 to +0.9	−1.0 to +1.1
scan speed, deg min^{-1}	4	variable	variable
data measd	5782	3292	3270
data $\lvert F\rvert^2 > 3\sigma\lvert F\rvert^2$	2257	2355	2083
ignorance factor	0.04	0.02	0.022

state materials is *intra*molecular or *inter*molecular in origin or a combination of both.

In the present study an effort was made to get an improved quantitative assessment for the *intra*molecular magnetic exchange interaction in the above complexes. Variable-temperature EPR data in the range of 3–12 K have been obtained for toluene–benzene glasses of five of the complexes. In addition, we report the results of single-crystal X-ray structural work on the mononuclear complex I and the binuclear com-

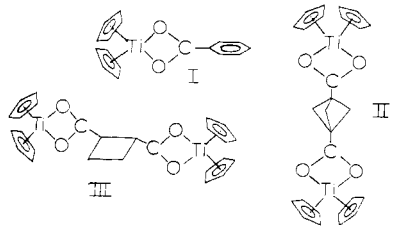

plexes II and III. The mononuclear benzoate complex (I) was selected for a structure determination because it is the only mononuclear complex studied that showed a magnetic exchange in the solid state.

Experimental Section

Compound Preparation. The general preparative procedures for the compounds studied in this investigation were reported previously.[3-5] Several samples of the benzoate compound $(\eta^5\text{-}C_5H_5)_2Ti(O_2CC_6H_5)$ were prepared, either via the reaction of $[(\eta^5\text{-}C_5H_5)_2TiCl]_2$ and $KO_2CC_6H_5$ in H_2O or via the reaction of $(\eta^5\text{-}C_5H_5)_2Ti(CO)_2$ and $HO_2CC_6H_5$ in THF. Samples of the benzoate compound were recrystallized from heptane, benzene–heptane, toluene–heptane, or xylene–heptane solutions.

A sample of $(\eta^5\text{-}C_5Me_5)_2Ti(O_2CC_6H_5)$ was synthesized by the reaction in an inert-atmosphere box of $(\eta^5\text{-}C_5Me_5)_2Ti(CO)_2$ and $HO_2CC_6H_5$ in THF see Table XXII for the analytical data[10]). No color change was noted after stirring the THF solution of these two reactants overnight at ambient temperatures. The solvent was removed under vacuum and the resulting brown powder was dissolved in heptane and filtered. The solution turned green after ~12 h, at which time the solvent was again removed under vacuum and the resulting blue powder dissolved in diethyl ether. Slow evaporation of this solution gave blue crystals.

(10) Supplementary material.

Table II. Positional Parameters[a] for $Cp_2TiO_2CC_6H_5$

atom	x	y	z
Ti(1)	0.38587 (9)	−0.41318 (9)	0.14030 (5)
Ti(2)	0.49518 (9)	0.08530 (9)	0.14219 (5)
O(1)	0.1915 (3)	−0.4301 (3)	0.1077 (2)
O(2)	0.2743 (3)	−0.2652 (3)	0.1412 (2)
C(1)	0.1806 (5)	−0.3248 (5)	0.1199 (3)
C(2)	0.0576 (3)	−0.2730 (5)	0.1101 (2)
C(3)	0.0468 (5)	−0.1658 (5)	0.1351 (3)
C(4)	−0.0685 (6)	−0.1183 (5)	0.1283 (3)
C(5)	−0.1694 (6)	−0.1775 (6)	0.0967 (3)
C(6)	0.1581 (5)	−0.2838 (6)	0.0707 (3)
C(7)	−0.0453 (5)	−0.3324 (5)	0.0779 (3)
C(8)	0.5515 (7)	−0.3947 (10)	0.0986 (4)
C(9)	0.4712 (11)	−0.3081 (6)	0.0728 (5)
C(10)	0.3687 (8)	−0.3663 (9)	0.0377 (4)
C(11)	0.3915 (9)	−0.4792 (8)	0.0444 (4)
C(12)	0.5008 (9)	−0.4962 (7)	0.0799 (4)
C(13)	0.3452 (7)	−0.4618 (12)	0.2325 (4)
C(14)	0.4292 (12)	−0.3857 (7)	0.2471 (4)
C(15)	0.5280 (8)	−0.4241 (9)	0.2352 (4)
C(16)	0.5094 (10)	−0.5318 (8)	0.2139 (3)
C(17)	0.3921 (13)	−0.5607 (8)	0.2106 (4)
O(3)	0.6157 (3)	0.2300 (3)	0.1447 (2)
O(4)	0.6453 (3)	0.0691 (3)	0.1018 (2)
C(18)	0.6793 (5)	0.1703 (5)	0.1175 (3)
C(19)	0.7906 (5)	0.2207 (5)	0.1060 (2)
C(20)	0.8498 (5)	0.1627 (5)	0.0687 (3)
C(21)	0.9523 (6)	0.2090 (6)	0.0568 (3)
C(22)	0.9993 (6)	0.3116 (6)	0.0852 (3)
C(23)	0.9414 (6)	0.3671 (5)	0.1224 (3)
C(24)	0.8369 (5)	0.3244 (5)	0.1332 (3)
C(25)	0.4414 (7)	−0.0249 (7)	0.2173 (3)
C(26)	0.4824 (8)	0.0800 (7)	0.2429 (3)
C(27)	0.6048 (8)	0.0881 (7)	0.2466 (3)
C(28)	0.6352 (7)	−0.0118 (9)	0.2214 (4)
C(29)	0.5343 (7)	−0.0812 (6)	0.2026 (3)
C(30)	0.2814 (5)	0.1108 (6)	0.1100 (3)
C(31)	0.3351 (6)	0.2030 (6)	0.0880 (3)
C(32)	0.3953 (6)	0.1588 (6)	0.0468 (3)
C(33)	0.3772 (6)	0.0392 (6)	0.0436 (3)
C(34)	0.3069 (5)	0.0074 (5)	0.0822 (3)

[a] Positional parameters are given as fractions of the unit cell edges. Estimated standard deviations of the least significant digits are given in parentheses.

Physical Measurements. Variable-temperature (4.2–286 K) magnetic susceptibility data were obtained with use of a Princeton Applied Research Model 150A vibrating-sample magnetometer operated at 13.5 kG. A calibrated GaAs diode was used for temperature determination. The magnetic susceptibility of $CuSO_4 \cdot 5H_2O$ was determined across the complete temperature range on several occasions, and these data were used as standards. Because all of the Ti(III) metallocenes are air sensitive, the samples for susceptibility determination were loaded into press-fit Kel-F sample cells in an inert-atmosphere box and introduced into the helium atmosphere of the magnetometer immediately after removal from the glovebox.

Variable-temperature (3–12 K) X-band EPR spectra were recorded for toluene–benzene (4:1) glasses at a power level of 0.0063 mW with a Bruker ER200 spectrometer in conjunction with an Oxford Instruments helium-flow accessory.[6] Temperature determination was effected with a carbon resistor. The error in the temperature determination at any point across the range of 3–12 K is estimated as ±0.1 K. Signal intensities of derivative-like features were approximated by peak-to-peak heights.[7,8] X-Band room-temperature powder spectra were measured with a Varian E-9 spectrometer. Powdered DPPH was used as a reference.

Structure Determination of the Benzoate "Monomer" $(\eta^5\text{-}C_5H_5)_2Ti(O_2CC_6H_5)$ (I). A crystal of $(\eta^5\text{-}C_5H_5)_2Ti(O_2CC_6H_5)$ (0.5 × 0.3 × 0.3 mm), which was sealed in a glass capillary tube, was mounted and aligned on a Syntex $P\bar{1}$ automated diffractometer. Photographs taken on the crystal indicated monoclinic symmetry; systematic absences observed in the intensity data indicated the space group $P2_1/n$. The centered settings of 25 reflections were used to

Table III. Positional Parameters[a] for $Cp_2TiO_2CC_5H_6CO_2TiCp_2$

atom	x	y	z
Ti	0.04460 (6)	0.11039 (4)	0.16116 (3)
O(1)	0.0106 (3)	0.3119 (2)	0.1485 (1)
O(2)	0.0544 (3)	0.2063 (2)	0.0553 (2)
C(1)	0.0264 (4)	0.3096 (2)	0.0809 (2)
C(2)	0.0103 (4)	0.4272 (3)	0.0314 (2)
C(3)	0.137 (2)	0.463 (1)	−0.006 (1)
C(4)	0.057 (2)	0.5649 (7)	0.0704 (6)
C(5)	−0.163 (1)	0.482 (1)	−0.0527 (8)
C(A1)	−0.2942 (6)	0.1243 (5)	0.1088 (5)
C(A2)	−0.2871 (6)	0.0843 (5)	0.0347 (3)
C(A3)	−0.1978 (6)	−0.0326 (5)	0.0588 (4)
C(A4)	−0.1554 (7)	−0.0582 (5)	0.1442 (4)
C(A5)	−0.2105 (7)	0.0316 (8)	0.1732 (4)
C(B1)	0.3800 (6)	0.0688 (9)	0.2174 (3)
C(B2)	0.3793 (6)	0.1680 (5)	0.2681 (4)
C(B3)	0.3104 (6)	0.1251 (4)	0.3178 (3)
C(B4)	0.2693 (5)	0.0026 (4)	0.3003 (3)
C(B5)	0.3110 (7)	−0.0328 (5)	0.2373 (4)

[a] Positional parameters are given as fractions of the unit cell edges. Estimated standard deviations of the least significant digits are given in parentheses.

calculate the cell constants given in Table I. Standard reflections monitored during data collection showed no significant deviations in intensity. The data were processed in the usual way, and the structure was solved with use of standard heavy-atom procedures. The final cycles of refinement converged with $R_F = 0.054$ and $R_{wF} = 0.059$. The error in an observation of unit weight was calculated to be 1.63. Computer programs, calculational procedures, and sources of scattering factor tables have been noted previously.[9] The final positional parameters for the principal atoms are given in Table II.

Structure Determination of the Bicyclo[1.1.1]pentane-1,3-dicarboxylate-Bridged Complex (η^5-$C_5H_5)_2Ti(O_2CC_5H_6CO_2)Ti(\eta^5$-$C_5H_5)_2$ (II). A deep blue crystal of $(\eta^5$-$C_5H_5)_2Ti(O_2CC_5H_6CO_2)$-$Ti(\eta^5$-$C_5H_5)_2$ (0.5 × 0.52 × 0.88 mm), which was sealed in a capillary tube, was mounted and aligned on a Syntex $P2_1$ automated diffractometer. Photographs taken on the crystal indicated monoclinic symmetry; systematic absences observed in the intensity data indicated the space group $P2_1/c$. The centered settings of 15 reflections were used to calculate the cell constants given in Table I. Standard reflections monitored during data collection showed no significant deviations in intensity. A conventional Patterson map revealed the position for the Ti atoms, and subsequent difference Fourier syntheses gave positions for all non-hydrogen atoms, the aromatic hydrogen atoms, and most of the disordered aliphatic hydrogen atoms. Two isotropic thermal coefficients were refined for the hydrogen atoms; one was applied to the aromatic group and the other to the disordered aliphatic group. All non-hydrogen atoms were varied with an anisotropic thermal coefficient. The largest change/error in the final least-squares cycle was 0.23, indicating convergence. The final difference Fourier was featureless, which confirms the proposed disorder model for the bridging ligand. The final values of the agreement factors R_F and R_{wF} were 0.044 and 0.061, respectively. The final positional parameters for the principal atoms are given in Table III.

Structure Determination of the *trans*-Cyclobutane-1,2-dicarboxylate-Bridged Complex (η^5-$C_5H_5)_2Ti(O_2CC_4H_6CO_2)Ti(\eta^5$-$C_5H_5)_2$ (III). A translucent blue crystal of $(\eta^5$-$C_5H_5)_2Ti$-$(O_2CC_4H_6CO_2)Ti(\eta^5$-$C_5H_5)_2$ (0.4 × 0.5 × 0.5 mm), which was sealed in a capillary tube, was mounted and aligned on a Syntex $P2_1$ automated diffractometer. Photographs taken on the crystal indicated orthorhombic symmetry, and a space group of $P2_12_12_1$ was assigned. The centered settings of 15 reflections were used to calculate the cell constants given in Table I. The solution was straightforward wherein a weighed (E^*F) Patterson synthesis revealed the positions for all of the remaining atoms, including all hydrogen atoms. All of the cyclopentadienyl hydrogen atoms were fixed in calculated positions. A single isotropic thermal coefficient was refined and applied to all 20 aromatic hydrogen atoms. All other hydrogen atoms were independently refined with anisotropic thermal motion. The largest change/error in the final cycle of least squares was 0.26, indicating all refined variables had converged. The final difference Fourier synthesis was completely featureless with a maximum residual electron density of 0.22 e Å^{-3}. The final values of the agreement factors R and R_w were found to be 0.038 and 0.052, respectively. Refinement of the enantiomer of the proposed structure converged with residuals of $R = 0.042$ and $R_w = 0.057$, which indicates our model was the correct choice. The final positional parameters for the principal atoms are given in Table IV.

Table IV. Positional Parameters[a] for $Cp_2TiO_2CC_4H_6CO_2TiCp_2$

atom	x	y	z
Ti(1)	0.01896 (7)	0.45821 (3)	−0.0425 (1)
Ti(2)	0.62520 (7)	0.31399 (3)	0.0911 (1)
O(1)	0.0262 (3)	0.3835 (1)	0.0611 (5)
O(2)	0.1812 (3)	0.4330 (1)	0.0806 (5)
O(3)	0.4345 (3)	0.3058 (1)	0.1357 (5)
O(4)	0.5263 (3)	0.3733 (1)	0.2123 (5)
C(1)	0.1966 (4)	0.3520 (2)	0.2078 (6)
C(2)	0.3186 (4)	0.3650 (2)	0.2904 (6)
C(3)	0.2751 (5)	0.3344 (3)	0.4427 (8)
C(4)	0.1450 (5)	0.3393 (3)	0.3803 (8)
C(5)	0.1330 (4)	0.3911 (2)	0.1121 (6)
C(6)	0.4310 (4)	0.3478 (2)	0.2083 (6)
C(A1)	0.0193 (6)	0.4096 (2)	−0.2882 (7)
C(A2)	−0.0624 (6)	0.4480 (3)	−0.3116 (7)
C(A3)	−0.0025 (8)	0.4925 (3)	−0.3109 (8)
C(A4)	0.1215 (7)	0.4820 (3)	−0.2877 (9)
C(A5)	0.1316 (6)	0.4301 (3)	−0.2736 (8)
C(B1)	−0.031 (1)	0.4839 (5)	0.2249 (9)
C(B2)	−0.1377 (9)	0.4692 (3)	0.151 (1)
C(B3)	−0.1591 (6)	0.5010 (3)	0.025 (1)
C(B4)	−0.071 (1)	0.5360 (3)	0.021 (1)
C(B5)	0.0105 (9)	0.5254 (4)	0.143 (2)
C(C1)	0.7183 (7)	0.2985 (3)	−0.1662 (8)
C(C2)	0.5982 (8)	0.2956 (3)	−0.1934 (8)
C(C3)	0.5512 (6)	0.3418 (3)	−0.1678 (8)
C(C4)	0.6397 (8)	0.3742 (3)	−0.1214 (9)
C(C5)	0.7458 (6)	0.3472 (3)	−0.1232 (9)
C(D1)	0.627 (1)	0.2700 (5)	0.344 (1)
C(D2)	0.706 (1)	0.3079 (5)	0.364 (1)
C(D3)	0.8000 (7)	0.2994 (4)	0.249 (1)
C(D4)	0.7721 (9)	0.2553 (4)	0.168 (1)
C(D5)	0.668 (1)	0.2388 (4)	0.225 (1)

[a] Positional parameters are given as fractions of the unit cell edges. Estimated standard deviations of the least significant digits are given in parentheses.

Listings of the thermal parameters, the observed and calculated structure factors, additional bond lengths and angles, and positional parameters of the hydrogen atoms for the three structures are available.[10]

Results and Discussion

The Benzoate Dilemma. An antiferromagnetic exchange interaction has been observed in the *solid state* for binuclear dicyclopentadienyltitanium(III) complexes with dicarboxylate, uracilate, imidazolate, and halide ion bridges (vide infra). It is clear from the titanium hyperfine patterns seen in room-temperature solution EPR spectra that some part of the interaction observed for these binuclear complexes is *intra*molecular in origin. The trends in the magnitude of the antiferromagnetic interaction in the solid state observed for various series of complexes also point to an *intra*molecular origin. For example, in the series of complexes bridged by ^-O_2C-$(CH_2)_nCO_2^-$ (n = 0–4, 6, 8, 10) dianions, the antiferromagnetic exchange interaction decreases monotonically as the value of n is increased.[3] An interaction was observed in magnetic susceptibility data measured down to 4.2 K for the first four members of the series, while no interaction was apparent for those binuclear complexes with four or more methylene carbon atoms in the bridge. In addition, no interaction was observed for several analogous mononuclear complexes in the solid state. Only one exception was found to the last statement. Magnetic susceptibility data for the supposedly monomeric benzoate complex $(\eta^5$-$C_5H_5)_2Ti(O_2CC_6H_5)$ gave clear evidence of the presence of an antiferromagnetic exchange interaction with $J = -4.0$ cm^{-1}.

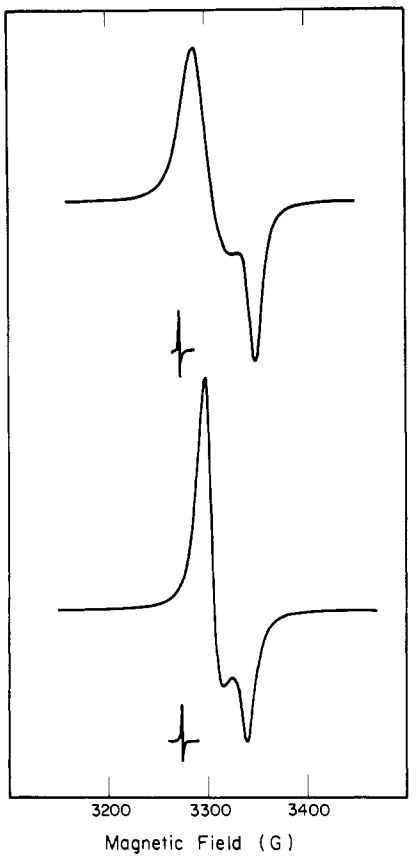

Figure 1. Room-temperature powder X-band EPR spectra for the benzoate complex $(\eta^5\text{-}C_5H_5)_2TiO_2CC_6H_5$ (I): large crystals (bottom) and microcrystals (top).

It is clear that the benzoate curiosity requires further study. As indicated in the Experimental Section, four new samples of the benzoate compound were prepared by recrystallization from four different solvent mixtures (see Table XXII[10]). For all four samples, variable-temperature magnetic susceptibility data[10] indicate antiferromagnetic exchange interactions of similar magnitude; a least-squares fit of the data sets to the dimer theoretical equation gave $-J = 3.7 \pm 0.3$ cm^{-1}.

EPR data were also collected for the above samples of the benzoate compound. Frozen-glass EPR spectra run for toluene–benzene (4:1) solutions of all of the samples were essentially identical, each giving a rhombic monomer signal with g values of 1.999, 1.982, and 1.950. At room temperature, a monomer-type signal[3-5] was seen for each solution with a g value of 1.98 and satellite hyperfine structure with an interline spacing of 8.5 G due to the presence of a small amount of titanium isotopes with a nonzero nuclear spin. In short, in dilute fluid or frozen solution there is no evidence in the EPR spectra of an intermolecular exchange. As can be seen in Figure 1, the spectrum obtained for the well-powdered sample from a large crystal is somewhat different than that obtained by thoroughly powdering microcrystalline, powder, and needlelike crystalline samples. It is very difficult to say what this means.

Analogues of the benzoate compound were prepared and studied (see Table XXII[10]). The titanium monomers with the anions of naphthalene-2-carboxylate $[(\eta^5\text{-}C_5H_5)_2Ti(O_2CC_{10}H_7)]$, 4-*tert*-butyl-benzoate $[(\eta^5\text{-}C_5H_5)_2Ti(O_2CC_6H_4C(CH_3)_3)]$, and biphenyl-4-carboxylate $[(\eta^5\text{-}C_5H_5)_2Ti(O_2C\text{-}C_6H_4\text{-}C_6H_5)]$ were synthesized and investigated by variable-temperature (4.2–286 K) magnetic susceptibility measurements. No magnetic exchange interaction was observed in the data[10] for these systems. The permethylated benzoate complex $(\eta^5\text{-}C_5Me_5)_2Ti(O_2CC_6H_5)$ was prepared, and it also exhibited no magnetic exchange interaction in the solid state. Crystal structures of the benzoate monomer (I) and two titanium dimers (II and III) were solved to elucidate the pathway for the exchange interaction operative in the benzoate monomer.

Structural Features of the Titanium Dimers. The principal intramolecular bond lengths and angles for $(\eta^5\text{-}C_5H_5)_2Ti(O_2CC_5H_6CO_2)Ti(\eta^5\text{-}C_5H_5)_2$ (II) and $(\eta^5\text{-}C_5H_5)_2Ti(O_2CC_4H_6CO_2)Ti(\eta^5\text{-}C_5H_5)_2$ (III) are given in Tables V and

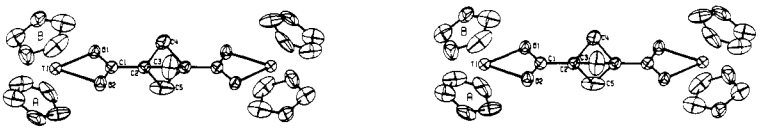

Figure 2. Stereographic drawing of the molecular structure of $(\eta^5\text{-}C_5H_5)_2TiO_2CC_5H_6CO_2Ti(\eta^5\text{-}C_5H_5)_2$. Hydrogen atoms are not included.

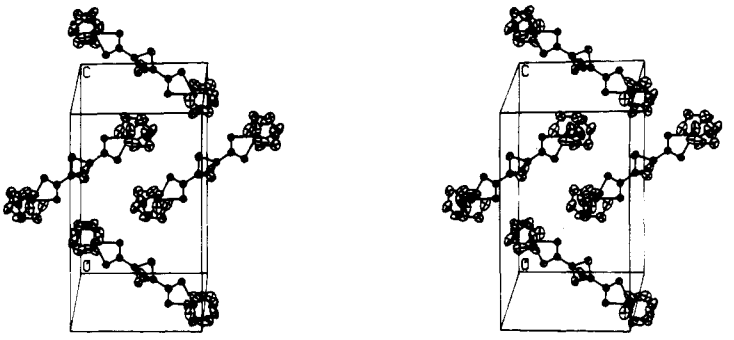

Figure 3. Stereographic drawing of the crystal packing in the unit cell of $(\eta^5\text{-}C_5H_5)_2TiO_2CC_5H_6CO_2Ti(\eta^5\text{-}C_5H_5)_2$.

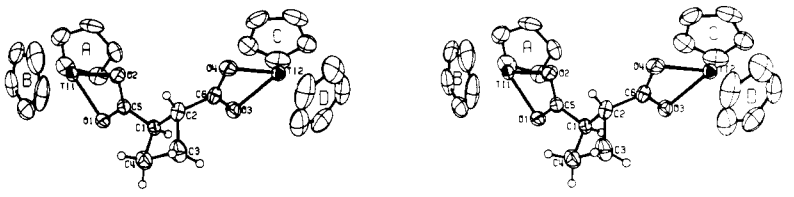

Figure 4. Stereographic drawing of the molecular structure of $(\eta^5\text{-}C_5H_5)_2TiO_2CC_4H_6CO_2Ti(\eta^5\text{-}C_5H_5)_2$.

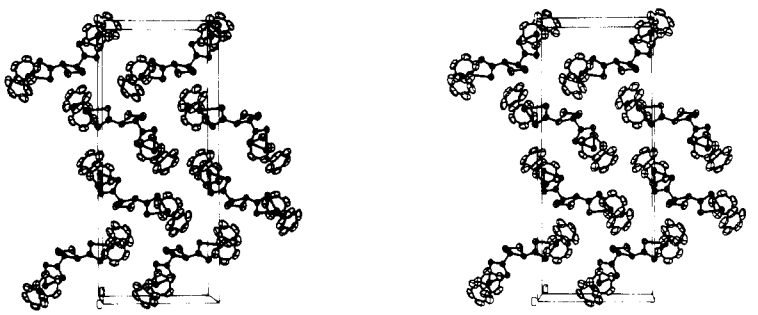

Figure 5. Stereographic drawing of the crystal packing in the unit cell of $(\eta^5\text{-}C_5H_5)_2TiO_2CC_4H_6CO_2Ti(\eta^5\text{-}C_5H_5)_2$.

Table V. Principal Bond Distances (Å) and Angles (deg) for the Ti Dimer Bridged by the Dianion Bicyclo[1.1.1]pentane-1,3-dicarboxylate, $Cp_2TiO_2CC_5H_6CO_2TiCp_2$

Ti-O(1)[a]	2.1635 (20)[b]	C(2)-C(3)	1.5511 (193)
Ti-O(2)	2.1622 (25)	C(2)-C(3')[c]	1.5538 (155)
Ti-Cp(A)	2.043 (6)	C(2)-C(4)	1.5748 (84)
Ti-Cp(B)	2.052 (5)	C(2)-C(4')	1.5458 (108)
O(1)-C(1)	1.2630 (40)	C(2)-C(5)	1.4681 (126)
O(2)-C(1)	1.2593 (35)	C(2)-C(5')	1.4488 (129)
C(1)-C(2)	1.4893 (39)		
O(1)-Ti-O(2)	60.38 (8)	C(1)-C(2)-C(4')	125.26 (57)
Cp(A)-Ti-Cp(B)	135.1 (2)	C(3)-C(2)-C(4)	84.16 (79)
O(1)-Ti-Cp(A)	109.1 (2)	C(3')-C(2)-C(4')	85.04 (79)
O(2)-Ti-Cp(A)	109.6 (2)	C(4)-C(2)-C(4')	106.95 (74)
O(1)-Ti-Cp(B)	109.6 (2)	C(1)-C(2)-C(5)	129.76 (54)
O(2)-Ti-Cp(B)	108.8 (2)	C(1)-C(2)-C(5')	129.35 (55)
Ti-O(1)-C(1)	90.14 (18)	C(2)-C(2)-C(5)	88.17 (78)
Ti-O(2)-C(1)	90.30 (19)	C(3')-C(2)-C(5')	88.76 (78)
O(1)-C(1)-O(2)	119.17 (29)	C(4)-C(2)-C(5)	85.69 (71)
O(1)-C(1)-C(2)	120.67 (27)	C(4')-C(2)-C(5')	87.44 (73)
O(2)-C(1)-C(2)	120.16 (28)	C(5)-C(2)-C(5')	100.89 (71)
C(1)-C(2)-C(3)	126.42 (63)	C(2)-C(3)-C(2')	73.49 (72)
C(1)-C(2)-C(3')	127.07 (63)	C(2)-C(4)-C(2')	73.05 (63)
C(3)-C(2)-C(3')	106.51 (85)	C(2)-C(5)-C(2')	79.11 (64)
C(1)-C(2)-C(4)	127.79 (56)		

[a] Refer to Figure 5 for the letter and number designations. [b] Standard deviations of the least significant figures are given in parentheses. [c] The primed atoms are symmetry generated from the corresponding unprimed atoms by the operation $-x$, $1.0-y$, $-z$.

Table VI. Principal Bond Distances (Å) and Angles (deg) for the Ti Dimer Bridged by the Dianion *trans*-Cyclobutane-1,2-dicarboxylate, $Cp_2TiO_2CC_4H_6CO_2TiCp_2$

Ti(1)-O(1)[a]	2.1706 (32)[b]	O(2)-C(5)	1.2692 (55)
Ti(1)-O(2)	2.1634 (35)	O(3)-C(6)	1.2690 (56)
Ti(1)-Cp(A)	2.0488 (63)	O(4)-C(6)	1.2603 (57)
Ti(1)-Cp(B)	2.0405 (101)	C(1)-C(2)	1.5479 (66)
Ti(2)-O(3)	2.1575 (32)	C(1)-C(4)	1.5400 (78)
Ti(2)-O(4)	2.1646 (35)	C(1)-C(5)	1.4807 (65)
Ti(2)-Cp(C)	2.0507 (70)	C(2)-C(3)	1.5518 (82)
Ti(2)-Cp(D)	2.0473 (102)	C(2)-C(6)	1.4852 (67)
O(1)-C(5)	1.2716 (53)	C(3)-C(4)	1.5340 (85)
O(1)-Ti(1)-O(2)	60.37 (13)	Ti(2)-O(4)-C(6)	90.80 (29)
O(1)-Ti(1)-Cp(A)	107.84 (21)	C(2)-C(1)-C(4)	89.31 (39)
O(2)-Ti(1)-Cp(A)	109.18 (21)	C(2)-C(1)-C(5)	118.71 (40)
O(1)-Ti(1)-Cp(B)	109.12 (30)	C(4)-C(1)-C(5)	116.61 (42)
O(2)-Ti(1)-Cp(B)	109.87 (30)	C(1)-C(2)-C(3)	87.02 (39)
Cp(A)-Ti(1)-Cp(B)	135.70 (34)	C(1)-C(2)-C(6)	118.24 (41)
O(3)-Ti(2)-O(4)	60.20 (13)	C(3)-C(2)-C(6)	116.64 (44)
O(3)-Ti(2)-Cp(C)	108.58 (23)	C(2)-C(3)-C(4)	89.38 (46)
O(4)-Ti(2)-Cp(C)	109.66 (23)	C(1)-C(4)-C(3)	87.93 (45)
O(3)-Ti(2)-Cp(D)	107.76 (31)	O(1)-C(5)-O(2)	118.10 (41)
O(4)-Ti(2)-Cp(D)	108.07 (31)	O(1)-C(5)-C(1)	119.89 (40)
Cp(C)-Ti(2)-Cp(D)	136.91 (36)	O(2)-C(5)-C(1)	121.99 (41)
Ti(1)-O(1)-C(5)	90.56 (26)	O(3)-C(6)-O(4)	117.97 (43)
Ti(1)-O(2)-C(5)	90.95 (28)	O(3)-C(6)-C(2)	120.43 (42)
Ti(2)-O(3)-C(6)	90.89 (27)	O(4)-C(6)-C(2)	121.57 (43)

[a] Refer to Figure 4 for the letter and number designations. [b] Standard deviations of the least significant figures are given in parentheses.

VI. Stereoscopic views of these two complexes and their unit cells are given in Figures 2–5.

The angles and distances within the titanium coordination sphere in both complexes agree with those of other structure determinations for $(\eta^5\text{-}C_5H_5)_2Ti^{III}O_2$ fragments.[11,12] The average carbon–carbon bond distance in the bridging unit of complex II is 1.534 (13) Å, which is close to that found in bicyclo[1.1.1]pentane.[13] Two of the C–CH_2–C angles in the bicyclopentane bridge (73.5 (7) and 73.0 (6)°) are similar to the average angle in bicyclo[1.1.1]pentane, while the third angle is significantly larger (79.1 (6)°). The nonbonding carbon–carbon bridgehead distance increases from 1.845 Å[14] in the hydrocarbon to 1.858 (4) Å in the titanium complex. The metallacycle (TiO_2C) is planar and perpendicular to the plane defined by Cp–Ti–Cp (see Table XXIII[10]). The intramolecular Ti–Ti distance is 9.8509 (6) Å, which agrees favorably with the 9.93-Å distance calculated[4] from the dipolar splitting in the frozen-glass EPR spectrum.

The carbon–carbon distances in the bridging unit of complex III are appropriate for single bonds (the average length is 1.543 (8) Å). The C(1)–C(2) bond length increases 0.031 (11) Å upon complex formation from the short distance of 1.517 (4) Å found in *trans*-1,2-cyclobutanedicarboxylic acid.[15] The cyclobutane ring is nonplanar (see Table XXIII[10]) with a dihedral angle between the planes defined by C(1)–C(2)–C(3) and C(1)–C(4)–C(3) of 153 (1)°. The two metallacycles are

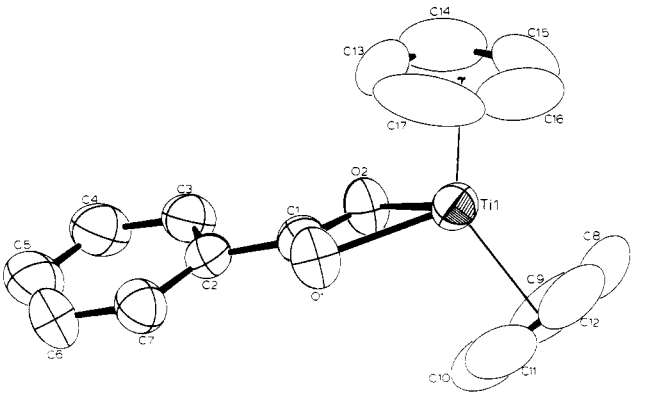

Figure 6. ORTEP plot of $(\eta^5\text{-}C_5H_5)_2TiO_2CC_6H_5$. Hydrogen atoms are not shown.

(11) Bottomley, F.; Lin, I. J. B.; White, P. S. *J. Organomet. Chem.* **1981**, *212*, 341.
(12) Fachinetti, G.; Floriani, C.; Chiesi-Villa, A.; Guastini, C. *J. Am. Chem. Soc.* **1979**, *101*, 1767.
(13) Chiang, J. F.; Bauer, S. H. *J. Am. Chem. Soc.* **1970**, *92*, 1614.
(14) No standard deviation is given; see ref 13.
(15) Benedetti, E.; Corradini, P.; Pedone, C. *Acta Crystallogr., Sect. B* **1970**, *B26*, 493.

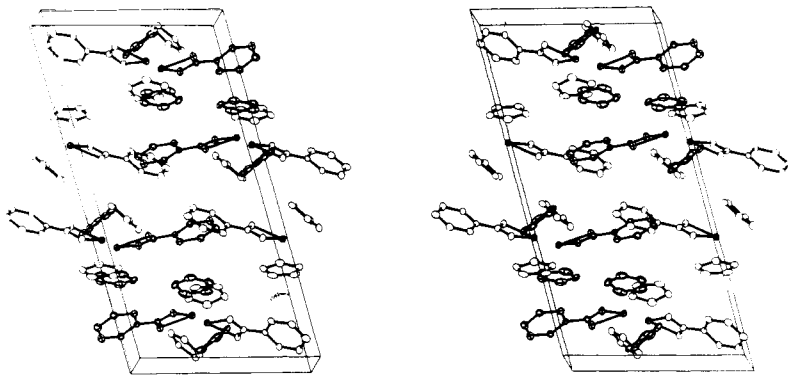

Figure 8. Stereographic drawing of the crystal packing in the unit cell of $(\eta^5\text{-}C_5H_5)_2TiO_2CC_6H_5$.

Table VII. Principal Bond Distances (Å) and Angles (deg) for the Benzoate Complex $Cp_2TiO_2CC_6H_5$

Ti(1)-O(1)[a]	2.152 (4)[b]	Ti(2)-O(3)	2.155 (3)
Ti(1)-O(2)	2.134 (3)	Ti(2)-O(4)	2.147 (3)
Ti(1)-Cp(A)	2.035 (9)	Ti(2)-Cp(C)	2.034 (7)
Ti(1)-Cp(B)	2.040 (8)	Ti(2)-Cp(D)	2.038 (7)
O(1)-C(1)	1.262 (6)	O(3)-C(18)	1.271 (5)
O(2)-C(1)	1.257 (6)	O(4)-C(18)	1.254 (6)
C(1)-C(2)	1.486 (7)	C(18)-C(19)	1.480 (7)
C(2)-C(3)	1.382 (7)	C(19)-C(20)	1.382 (7)
C(3)-C(4)	1.394 (7)	C(20)-C(21)	1.374 (7)
C(4)-C(5)	1.369 (8)	C(21)-C(22)	1.389 (9)
C(5)-C(6)	1.385 (8)	C(22)-C(23)	1.359 (9)
C(6)-C(7)	1.373 (7)	C(23)-C(24)	1.367 (7)
C(7)-C(2)	1.389 (7)	C(24)-C(19)	1.389 (7)
Cp(A)-Ti(1)-Cp(B)	136.0 (4)	Cp(C)-Ti(2)-Cp(D)	135.1 (3)
O(1)-Ti(1)-Cp(A)	108.2 (3)	O(3)-Ti(2)-Cp(C)	107.8 (3)
O(1)-Ti(1)-Cp(B)	109.3 (3)	O(3)-Ti(2)-Cp(D)	111.2 (2)
O(2)-Ti(1)-Cp(A)	110.6 (3)	O(4)-Ti(2)-Cp(C)	109.2 (2)
O(2)-Ti(1)-Cp(B)	107.1 (3)	O(4)-Ti(2)-Cp(D)	108.7 (2)
O(1)-Ti(1)-O(2)	60.9 (1)	O(3)-Ti(2)-O(4)	60.5 (1)
Ti(1)-O(1)-C(1)	89.4 (3)	Ti(2)-O(3)-C(18)	90.2 (3)
Ti(1)-O(2)-C(1)	90.3 (3)	Ti(2)-O(4)-C(18)	91.0 (3)
O(1)-C(1)-O(2)	119.3 (5)	O(3)-C(18)-O(4)	118.2 (5)
O(1)-C(1)-C(2)	119.9 (5)	O(3)-C(18)-C(19)	119.7 (5)
O(2)-C(1)-C(2)	120.7 (5)	O(4)-C(18)-C(19)	122.1 (5)
C(1)-C(2)-C(3)	118.7 (5)	C(18)-C(19)-C(20)	119.6 (5)
C(1)-C(2)-C(7)	120.8 (5)	C(18)-C(19)-C(24)	120.4 (5)
C(3)-C(2)-C(7)	120.4 (5)	C(20)-C(19)-C(24)	120.1 (5)
C(2)-C(3)-C(4)	119.3 (5)	C(19)-C(20)-C(21)	120.4 (6)
C(3)-C(4)-C(5)	120.0 (6)	C(20)-C(21)-C(22)	119.0 (6)
C(4)-C(5)-C(6)	120.5 (6)	C(21)-C(22)-C(23)	120.0 (7)
C(5)-C(6)-C(7)	120.0 (6)	C(22)-C(23)-C(24)	121.7 (6)
C(6)-C(7)-C(2)	119.7 (6)	C(23)-C(24)-C(19)	118.7 (6)

[a] Refer to Figures 9 and 10 for the number designations. The letter designations for the cyclopentadienyl rings are as follows: Cp(A), C(8)-C(12); Cp(B), C(13)-C(17); Cp(C), C(25)-C(29); Cp(D), C(30)-C(34). [b] Standard deviations of the least significant figures are given in parentheses.

planar, and the angle between the normals to these two planes is 56 (1)°. The internal rotation angle, C(5)-C(1)-C(2)-C(6), is 102.1 (5)° as compared to 99.1 (2)° in the hydrocarbon. The intramolecular Ti-Ti vector in the dimer is 7.8326 (11) Å. The poor agreement of this value with the 8.25-Å distance calculated[4] from the frozen-glass EPR spectrum was anticipated due to the low symmetry of the titanium complex.

Structure of the Benzoate Monomer. The principal intramolecular bond lengths and angles for $(\eta^5\text{-}C_5H_5)_2TiO_2CC_6H_5$ (I) are given in Table VII. ORTEP views of the two independent molecules in the unit cell are given in Figures 6 and 7.[10] A stereoscopic view of the unit cell is given in Figure 8. The distances and angles in the titanium coordination sphere are normal. The average angle and bond length in the phenyl moiety are 120.0 (6)° and 1.379 (8) Å, respectively. The planes of the benzene ligands are tipped 12.8 and 11.3° relative to the planes of the metallacycles in molecules 1 and 2, respectively (see Table XXIII[10]). There is no stacking of the phenyl rings observed in the packing diagram. The rings are tilted with an angle of 38.5° relative to one another, and the closest approach between the rings, atoms C(4) and C(20), is 3.6 Å.

Table VIII. Hydrogen-Bonding Interactions[a]

complex	C-O, Å	C-H[b]-O, deg	C-Ti, Å	C-H-Ti, deg
$Cp_2TiO_2CC_6H_5$	3.482 (7)	159.5	5.06	146.6
$Cp_2TiO_2CC_5H_6CO_2TiCp_2$	3.383 (6)	171.7	4.75	148.5
$Cp_2TiO_2CC_4H_6CO_2TiCp_2$	3.331 (8)	150.7	4.76	138.6
	3.511 (9)	169.0	5.34	168.4
	3.451 (9)	176.1	4.81	153.2

[a] The specific atoms examined are as follows: $Cp_2TiO_2CC_6H_5$ H(34), C(34), O(2), Ti(1); $Cp_2TiO_2CC_5H_6CO_2TiCp_2$ H(A3), C(A3), O(2), Ti; $Cp_2TiO_2CC_4H_6CO_2TiCp_2$ (H(A4), C(A4), O(2), Ti(1)), (H(B4), C(B4), O(4), Ti(2)), (H(D4), C(D4), O(3), Ti(2)). [b] The hydrogen atoms were fixed at a distance 0.95 Å from the corresponding carbon atom.

Possible Intermolecular Interactions. *Inter*molecular interactions of the dipolar and/or magnetic exchange type have been observed between monomeric complexes in the solid state.[16-19] These interactions have been reported to be on the order of 10^{-2} cm^{-1} for monomeric complexes with metal-metal separations of 4.8 Å. The $J = -4$ cm^{-1} antiferromagnetic exchange interaction observed in the solid state for the benzoate complex (I) cannot result solely from dipolar interactions. A dipolar interaction of this magnitude would require an intermolecular Ti-Ti distance less than 1 Å. The packing diagrams of the three complexes, I-III, have been examined to identify the pathway(s) responsible for the magnetic exchange interaction observed in the solid state for the benzoate complex. Three different types of interactions were investigated in detail: a direct Ti-Ti interaction, a Ti-O···Ti interaction, and hydrogen-bonding contacts involving either Ti-O···H-C-Ti or Ti-C-H···Ti.

Examination of the packing diagrams for the three molecules revealed no significant hydrogen-bonding interactions. The pertinent distances and angles are listed in Table VIII. The carbon-oxygen distances of the Ti-O···H-C-Ti pathway are longer than the distances reported for similar types of hydrogen-bonding contacts observed in organic systems.[20,21] The relatively long titanium-carbon distances in the Ti-C-H···Ti pathway also preclude appreciable *inter*molecular ex-

(16) Addison, A. W.; Burke, P. J.; Henrick, K. *Inorg. Chem.* **1982**, *21*, 60.
(17) Barker, P. J.; Stobart, S. R. *J. Chem. Soc., Chem. Commun.* **1980**, *969*.
(18) Simpson, G. D.; Belford, R. L.; Biagioni, R. *Inorg. Chem.* **1978**, *17*, 2424.
(19) So, H.; Haight, G. P.; Belford, R. L. *J. Phys. Chem.* **1980**, *84*, 1849.
(20) Sutor, D. J. *Nature (London)* **1962**, *195*, 68.
(21) Hamilton, W. C.; Ibers, J. A. In "Hydrogen Bonding in the Solids"; W. A. Benjamin: New York, 1968.

Table IX. Titanium-Titanium and Titanium-Oxygen Interactions[a]

complex	Ti-O,[b] Å	Ti-O-Ti, deg	Ti-Ti, Å	Ti-Ti-Ti, deg
$Cp_2TiO_2CC_6H_5$	4.767	111.5	5.895	156
	4.873	108.8	5.929	
$Cp_2TiO_2CC_5H_6CO_2TiCp_2$	4.801	106.0	5.783	
$Cp_2TiO_2CC_4H_6CO_2TiCp_2$	4.829	110.0	5.932	

[a] The specific atoms examined are as follows: $Cp_2TiO_2CC_6H_5$ Ti(1), O(2), Ti(2), O(3); $Cp_2TiO_2CC_5H_4CO_2TiCp_2$ Ti, O(2), Ti ($-x, -y, -z$); $Cp_2TiO_2CC_4H_5CO_2TiCp_2$ Ti(1), O(1), Ti(2) ($-1 + x, y, z$). [b] Only the intermolecular distances are given. See Tables V-VII for the intramolecular Ti-O distances.

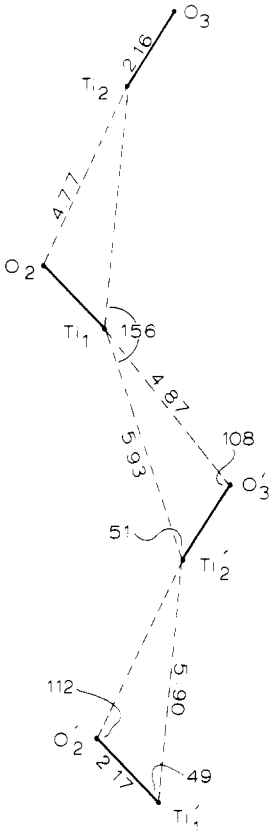

Figure 9. Plane containing the extended interaction in $(\eta^5\text{-}C_5H_5)_2TiO_2CC_6H_5$. The distances are given in units of angstroms, and the angles are given in units of degrees.

change interactions. Both of these hydrogen-bonding contact pathways involve a cyclopentadienyl C–H fragment. The fact that the unpaired electron is in a titanium orbital that is nonbonding toward the cyclopentadienyl ligand also does not bode well for these pathways serving as viable pathways for even a weak exchange interaction.

An interesting difference in intermolecular packing was noted between the benzoate complex I and the two binuclear complexes II and III. Complexes II and III in the solid state exhibit pairwise (i.e., involve only two Ti ions) associations between two binuclear complexes. Each of these pairwise associations involve a Ti–O···Ti contact with Ti···O $\simeq$ 4.8 Å and a Ti···Ti contact of ~5.9 Å. This same type of pairwise association is seen for the benzoate complex; however, the association is extended in one dimension. The two independent benzoate molecules pack in the unit cell such that the Ti(1), O(2), Ti(2), and O(3) atoms define a plane that extends along the crystallographic *b* axis. This plane and the pertinent distances and angles are shown in Figure 9 (see Table IX).

The magnetic susceptibility data for the benzoate monomer I were fit to the Heisenberg model for isotropic antiferromagnetic exchange in linear chains. The polynomial employed to fit the data is given in eq 1, where $X = kT/|J|$.[22] The data

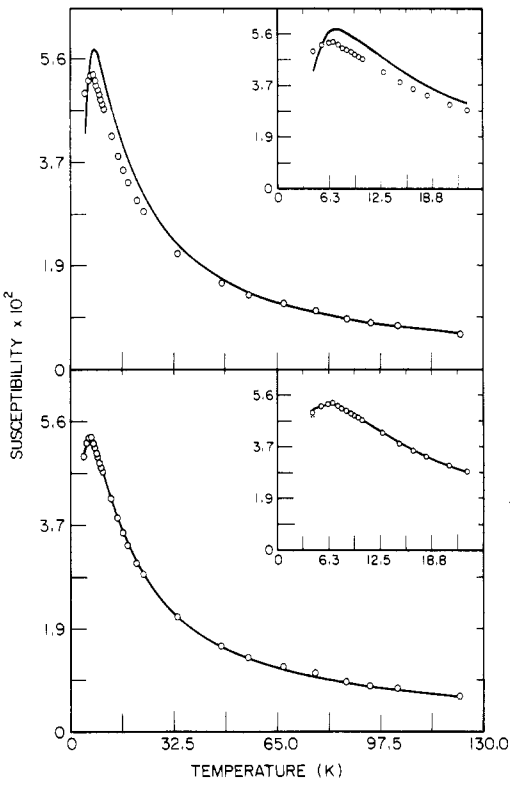

Figure 10. Plots of the molar paramagnetic susceptibility of two molecular units vs. temperature for $(\eta^5\text{-}C_5H_5)_2TiO_2CC_6H_5$. The data are least-squares fit to the Bleaney–Bowers equation (top) and to an equation for a chain model (bottom); see the text for an explanation.

$$\chi = \frac{Ng^2\beta^2}{kT}\,\frac{0.250 + 0.14995X^{-1} + 0.30094X^{-2}}{1 + 1.9862X^{-1} + 0.68854X^{-2} + 0.0626X^{-3}} \quad (1)$$

were least-squares fit to give an exchange parameter of -3.3 cm^{-1}. The data were previously least-squares fit[5] to the Bleaney–Bowers equation for a $S_1 = S_2 = {}^1/_2$ dimer to give an exchange parameter of -4.0 cm^{-1}. A comparison of the two fits is shown in Figure 10 (see Table XXIV[10]). The linear-chain model more accurately describes the data below 20 K, which supports the extended interactions as the pathway for the exchange interactions.

It is possible that there is a pronounced temperature dependence in the structure of the benzoate complex and at low temperature a different packing arrangement may exist in which the benzoate monomers have the appropriate orientation and interaction to propagate magnetic exchange. Several examples of pronounced temperature dependence of exchange parameters have been cited in the literature.[23-25]

Variable-Temperature EPR. The exchange parameter measured in the solid state can have contributions from both *intra*molecular (i.e., through the saturated hydrocarbon bridge) and *inter*molecular magnetic exchange interactions. Variable-temperature (3–12 K) EPR measurements were made for magnetically dilute frozen glasses of several of the complexes to assess the magnitude of the *intra*molecular magnetic exchange interaction.

(22) Estes, W. E.; Hatfield, W. E.; van Ooijen, J. A. C.; Reedjik, J. *J. Chem. Soc., Dalton Trans.* **1980**, 2121.
(23) Duggan, D. M.; Hendrickson, D. N. *Inorg. Chem.* **1974**, *13*, 2929.
(24) Kahn, O.; Morgenstern-Badarau, I.; Audiere, J. P.; Lehn, J. M.; Sullivan, S. A. *J. Am. Chem. Soc.* **1980**, *102*, 5935.
(25) Mikuriya, M.; Okawa, H.; Kida, S. *Bull. Chem. Soc. Jpn.* **1981**, *54*, 2979.

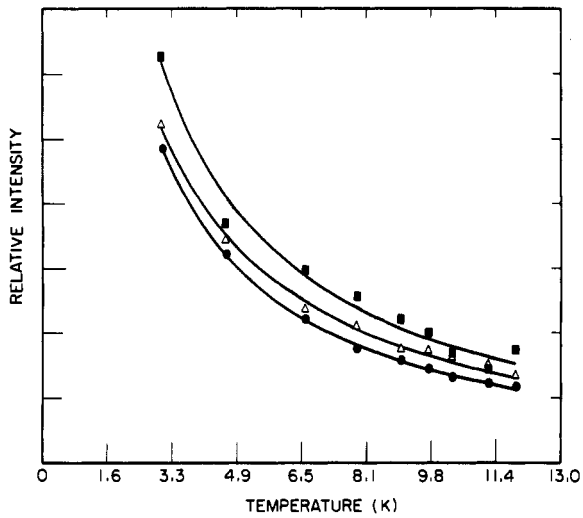

Figure 11. Experimental plots of relative intensity (arbitrary units), I, vs. temperature for compounds IV (●), V (■), and VI (△). The lines represent the theoretical fit to eq 2.

In the titanium dimers there are two thermally accessible spin states: the triplet excited state and the single ground state. The energy difference between these two states is $-2J$. The triplet state can be depopulated by lowering the temperature, which leads to a decrease in the intensity of the EPR signal. By examining the signal intensity in a dilute frozen glass as a function of temperature, it is possible to assess the intramolecular component of the exchange parameter. The titanium dimers bridged by the dianions malonate (IV), glutarate (V), adipate (VI), and sebacate (VII) and the monomer with adamantane-1-carboxylate (VIII) as the ligand were studied.[26] The temperature dependence of the intensity of the $\Delta M_s = 2$ transition was examined for dimers IV–VI. Because no $\Delta M_s = 2$ transition is observed for dimer VII and monomer VIII, the $\Delta M_s = 1$ region of the spectrum was examined. The data were least-squares fit to eq 2, where I is the intensity and C is a constant.[27]

$$I = (C/T)[3 + \exp(-2J/kT)]^{-1} \quad (2)$$

Before discussing our results, it is necessary to mention that there are several experimental difficulties inherent in EPR experiments performed on complexes dissolved in glasses in the temperature range of 3–12 K. Particular attention has been paid to a reasonably accurate determination of sample temperature, reproducible sample positioning, the temperature dependence of the cavity Q factor, the formation of good glasses, and power saturation effects.

Saturation of the $\Delta M_s = 1$ EPR signal of complexes VII and VIII could not be avoided. Even at the lowest microwave power level (5×10^{-5} mW) that gave a reasonable spectrum, saturation of the EPR signal for these two complexes was observed. The presence of power saturation was confirmed by examining the signal intensity as a function of the microwave power. In the absence of saturation effects a linear relationship between the signal intensity and the square root of the microwave power is expected.[28] The $\Delta M_s = 2$ signals seen for dimers IV–VI did *not* show power saturation effects. As a consequence, it was concluded that only for complexes IV–VI could we use EPR intensities in the range of 3–12 K to gauge *intra*molecular exchange interactions in a magnetically dilute glass medium.

The relative intensities of $\Delta M_s = 2$ transitions as a function of temperature are shown in Figure 11 for complexes IV–VI. These data were least-squares fit to eq 2 to give J values of -0.37, -0.42, and -0.56 cm^{-1}, respectively (see Table XXV[10]). It is estimated that the error on each of these J values could be as large as ± 0.3 cm^{-1}. It is clear that there is an *intra*molecular magnetic exchange interaction present in these three complexes; however, J values cannot accurately be determined with this technique.

Conclusion and Comments

In our previous papers[3-5] the presence of *intra*molecular magnetic exchange interactions in binuclear titanium(III) metallocenes was definitely established via the titanium hyperfine structure that is seen in room-temperature solution EPR spectra. This means that $|J| >> 0.001$ cm^{-1} for each of the complexes. Several of the bridges in the complexes that showed titanium hyperfine have saturated chains of methylene carbon atoms, including the following dicarboxylate dianions: adamantane-1,3-dicarboxylate, *trans*-cyclohexane-1,4-dicarboxylate, bicyclo[1.1.1]pentane-1,3-dicarboxylate, succinate, 2-methyl-2-ethylsuccinate, 3,3-diethylglutarate, and adipate.

In the present paper the solid-state structures of two of the dicarboxylate-bridged binuclear titanium(III) metallocenes have been determined to be as proposed. The nature of the antiferromagnetic exchange interaction ($-J = 1$–4 cm^{-1}) seen in the solid state for several of these complexes was reinvestigated. It was of importance to establish whether these interactions are totally *intra*molecular or are part *inter*molecular and part *inter*molecular in origin—a difficult task. At the outset of this work it seemed that only the ($J = -4.1$ cm^{-1}) antiferromagnetic interaction observed for the benzoate "monomer", $(\eta^5\text{-}C_5H_5)_2Ti(O_2CC_6H_5)$, stood in the way of saying that the interactions seen for the binuclear complexes in the solid state are due to *intra*molecular interactions. After all, six other analogous monomeric complexes that we prepared did *not* show such an antiferromagnetic exchange interaction. However, the X-ray structure of the benzoate complex showed that it is "monomeric" in the solid state. The packing diagram of the benzoate complex was examined, and a probable extended pathway for *inter*molecular magnetic exchange interactions was identified. The presence of an appreciable *inter*molecular interaction in the benzoate "monomer" makes it likely that the exchange parameters measured[3-5] in the solid state for the weakly interacting binuclear titanium(III) metallocenes bridged by dicarboxylate dianions have an intermolecular contribution. However, the decrease in intensity of the $\Delta M_s = 2$ EPR signal as a function of temperature (3–12 K) observed in this work for the malonate-, glutarate-, and adipate-bridged complexes supports the proposal that there is an appreciable *intra*molecular interaction.

There can be no question about the presence of *intra*molecular magnetic exchange interactions in several other[29,30,33-37]

(26) The molecular formulas of the titanium complexes are as follows: $(\eta^5\text{-}C_5H_5)_2Ti(O_2CCH_2CO_2)Ti(\eta^5\text{-}C_5H_5)_2$ (IV), $(\eta^5\text{-}C_5H_5)_2Ti(O_2C(CH_2)_3CO_2)Ti(\eta^5\text{-}C_5H_5)_2$ (V), $(\eta^5\text{-}C_5H_5)_2Ti(O_2C(CH_2)_4CO_2)Ti(\eta^5\text{-}C_5H_5)_2$ (VI), $(\eta^5\text{-}C_5H_5)_2Ti(O_2C(CH_2)_8CO_2)Ti(\eta^5\text{-}C_5H_5)_2$ (VII), and $(\eta^5\text{-}C_5H_5)_2TiO_2CC_{10}H_{15}$ (VIII).

(27) Poole, C. P. In "Electron Spin Resonance: a Comprehensive Treatise on Experimental Techniques"; Interscience: New York, 1967; p 555.

(28) Wertz, J. E.; Bolton, J. R. Reference 7, p 456.

(29) Coutts, R. S. P.; Wailes, P. C.; Martin, R. L. *J. Organomet. Chem.* **1973**, *47*, 375.

(30) Jungst, R.; Sekutowski, D.; Davis, J.; Luly, M.; Stucky, G. *Inorg. Chem.* **1977**, *16*, 1645.

(31) Kolks, G.; Lippard, S. J.; Waszczak, J. V.; Lilienthal, H. R. *J. Am. Chem. Soc.* **1982**, *104*, 717.

(32) Haddad, M. S.; Duesler, E. N.; Hendrickson, D. N. *Inorg. Chem.* **1979**, *18*, 141. Haddad, M. S.; Hendrickson, D. N. *Ibid.* **1978**, *17*, 2622.

(33) Jungst, R.; Sekutowski, D.; Stucky, G. *J. Am. Chem. Soc.* **1974**, *96*, 8108.

(34) Fieselmann, B. F.; Hendrickson, D. N.; Stucky, G. D. *Inorg. Chem.* **1978**, *17*, 1841.

(35) Sekutowski, D.; Jungst, R.; Stucky, G. D. *Inorg. Chem.* **1978**, *17*, 1848.

(36) Fieselmann, B. F.; Hendrickson, D. N.; Stucky, G. D. *Inorg. Chem.* **1978**, *17*, 2078.

binuclear titanium(III) metallocenes. Moderately strong antiferromagnetic interactions have been observed[30] for the halide-bridged complexes $[(\eta^5\text{-}C_5H_4CH_3)_2TiX]_2$, where J is -160 cm^{-1} for X = Cl$^-$ and -138 cm^{-1} for X = Br$^-$. A weaker interaction was found[33] for the bridged complexes of the composition $[(\eta^5\text{-}C_5H_5)_2Ti]_2MCl_4$:

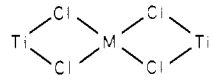

where $J = -8.9$ cm^{-1} for M = Zn and -6.9 cm^{-1} for M = Be. In view of recent work[31,32] that has demonstrated the viability of imidazolate-like bridges for the propagation of σ-pathway magnetic exchange interactions, it is reasonable that the 2,2′-biimidazolate- ($J = -25$ cm^{-1}) and 2,2′-bibenzimidazolate-bridged ($J = -19.2$ cm^{-1}) binuclear titanium(III) metallocenes have interactions that are intermediate between those of the above two types of complexes.[36] The dianionic bridge in this type of complex has the structure

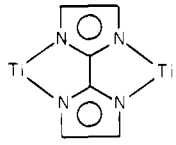

Weak antiferromagnetic ($-J = -1$ to -3 cm^{-1}) and ferromagnetic ($J \simeq 2$ cm^{-1}) interactions were also noted for a large number of binuclear titanium(III) metallocenes bridged by a variety of heterocyclic moieties.[34,37,38] The bridges in this last class included the dianions of hydroxyquinoxalines (A),

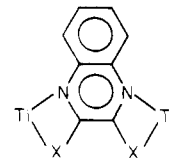

A, X = O, S

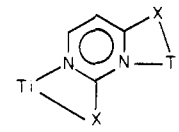

B, X = O, S

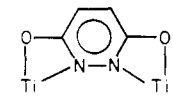

C

pyrimidines (B), and hydroxypyridazines (C). In all of the above complexes the $(\eta^5\text{-}C_5H_5)_2Ti^{III}$ moiety has a single unpaired electron in an orbital that is nonbonding relative to the cyclopentadienyl ligands and is poised for a σ type of overlap with the orbitals of a bridging species. To first order, then, the *intra*molecular magnetic exchange interactions are propagated by a σ exchange pathway.

Acknowledgment. The support of the National Institutes of Health under Grant HL 13652 is gratefully acknowledged. The X-ray diffraction equipment and the Bruker X-band EPR spectrometer were purchased in part by departmental NSF grants.

Registry No. I, 12248-57-6; II, 77071-27-3; III, 84098-55-5; $(\eta^5\text{-}C_5Me_5)_2TiO_2CC_6H_5$, 84098-56-6; $(\eta^5\text{-}C_5H_5)_2TiO_2CC_{12}H_9$, 84108-20-3; $(\eta^5\text{-}C_5H_5)_2TiO_2CC_{10}H_7$, 84098-57-7; $(\eta^5\text{-}C_5H_5)_2TiO_2CC_{10}H_{13}$, 84098-58-8.

Supplementary Material Available: An ORTEP plot of $(\eta^5\text{-}C_5H_5)_2TiO_2CC_6H_5$ (Figure 7) and listings of anisotropic (Table X) and isotropic (Table XI) thermal parameters, additional distances and angles (Tables XII–XIV), additional positional parameters (Tables XV–XVII), thermal parameters (Tables XVIII and XIX), experimental magnetic moments (Tables XX and XXI), analytical data (Table XXII), best planes and deviations of atoms (Table XXIII), experimental and calculated magnetic susceptibility data (Table XXIV) and EPR signal intensities (Table XXV) and observed and calculated structure factors (54 pages). Ordering information is given on any current masthead page.

(37) Francesconi, L. C.; Corbin, D. R.; Hendrickson, D. N.; Stucky, G. D. *Inorg. Chem.* **1979**, *18*, 3074.
(38) Corbin, D. R.; Francesconi, L. C.; Hendrickson, D. N.; Stucky, G. D. *Inorg. Chem.* **1981**, *20*, 2084.